Analysis of GPR Early-Time Signal Features for the Evaluation of Soil Permittivity Through Numerical and Experimental Surveys

Davide Comite, *Member, IEEE*, Alessandro Galli, *Member, IEEE*, Sebastian Emanuel Lauro, Elisabetta Mattei, and Elena Pettinelli

***Abstract*—Recently, various studies have been carried out in order to address the possible relationships between amplitude attributes of the "first-arrival direct wave" (the so-called "early-time signal," ETS), propagating at the interface in bistatic ground-penetrating radar (GPR) configurations, and the relevant shallow-soil permittivity parameters (dielectric constant and conductivity). In this frame, *ad hoc* compared numerical analyses and experimental investigations are extensively developed and discussed here, with the aim of making clearer the distinctive features and the reliability of this technique. The accurate results achieved for the ETS behavior as a function of various GPR system parameters enable us to identify both which are the more revealing signal attributes able to give predictable correlation with the ground permittivity values and the degree of complexity of the functional relationships between ETS amplitude and system parameters. A number of indications and perspectives are, thus, outlined in order to elucidate features, potential and critical aspects of the ETS technique for effective geophysical applications.**

***Index Terms*—Bistatic antenna features, early-time signal (ETS), ground-penetrating radar (GPR), signal waveforms, soil permittivity.**

I. Introduction and Background

GROUND-PENETRATING radar (GPR) represents a well-assessed and widely used technique commonly employed for nondestructive testing (NDT) in a variety of geophysical, planetary, civil, and environmental applications, with the main aim of locating and imaging hidden targets via electromagnetic (EM) sounding [1]–[5].

It is also known that several techniques using GPR have been proposed in the literature in order to evaluate the permittivity of subsoil for various types of geophysical applications. In low-loss nonmagnetic media, typical bistatic configurations of GPR have been proposed to estimate properties of the shallow subsurface dependent on the permittivity (e.g., water content [6]–[10]) by measuring the velocity of the "ground wave," either with common-mid-point (CMP) or with wide-angle-reflection-and-refraction (WARR) techniques at a medium interface [11]–[14]. It is noted, however, that such ground-coupled "multioffset" configurations are quite time consuming, have various limitations in the spatial resolution, and, above all, are applicable only with fully bistatic radar systems equipped with detachable transmitting (Tx) and receiving (Rx) antennas.

In this context, a novel opportunity has recently received attention, which is potentially more efficient and straightforward with respect to the above-mentioned canonical techniques for soil mapping. In fact, the use of a simple GPR configuration with close fixed ground-coupled antennas allows for the evaluation of the instantaneous amplitude of that portion of the signal where the interfacial "air" and "ground" waves partially overlap and are not still clearly separated: this first-arrival direct wave is the so-called "early-time signal" (ETS) [15]–[17]. Indeed a number of studies, particularly in the last years, observed systematic differences of the GPR direct-wave peak-to-peak amplitude varying, e.g., with the degree of saturation of concrete [18], [19]. It is expected that changes in amplitude, shape, and time duration of the GPR received signal should occur, since the ground-coupled antenna parameters are sensitively affected by the EM properties of the underlying media and by the overall environment [1]–[5], [16], [17]. Nevertheless, the relationships between the medium properties and the characteristics of the ETS are difficult to establish, even though a number of subsequent investigations showed some clear tendencies [20]–[27]. In particular, with close ground-coupled antennas, a high degree of correlation was found between the shallow-soil permittivity and the ETS amplitude. It was experimentally tested that a variation of the medium dielectric constant influences the amplitude, the shape, and the duration of the first-arrival GPR signals, whereas a variation of the medium conductivity influences mainly the ETS amplitude [15]–[17].

Theoretical analyses could confirm these overall behaviors, even though a number of significant approximations and simplifications were necessarily required in the EM problem modeling: in [16], e.g., it was observed that the received ETS amplitude could be approximated using an inverse function of the subsurface relative dielectric constant ε_r. Nevertheless, there is a complex dependence of the signal characteristics on the GPR scenario that can be chosen, involving the type and radiative properties of the antennas, the setup geometry

Manuscript received December 29, 2014; revised May 12, 2015; accepted July 28, 2015.

D. Comite and A. Galli are with the Department of Information Engineering, Electronics, and Telecommunications (DIET), Sapienza University, Rome 00184, Italy (e-mail: comite@diet.uniroma1.it).

S. E. Lauro and E. Pettinelli are with the Department Mathematics and Physics, Roma Tre University, Rome 00146, Italy.

E. Mattei is with the Department of ecological and biological science, University of Tuscia, Viterbo 01100, Italy.

Color versions of one or more of the figures in this paper are available online at http://ieeexplore.ieee.org.

Digital Object Identifier 10.1109/JSTARS.2015.2466174

(e.g., the location of the Tx/Rx elements), the features of the transmitted signal waveform and relevant frequency spectrum, the EM contrast between the upper and lower media, and their dispersion and loss effects [28]. If an effective quantitative assessment of the technique is searched for, it looks, therefore, essential to investigate such problem extensively by means of accurate EM experimental laboratory and also numerical techniques.

The objective of this paper is to analyze these issues with efficient and reliable means. Actually, most of the previous work developed by the same authors and other researchers on such topic (see, e.g., [15]–[27]) have been focused on different investigations of experimental nature. A systematic parametric study seems necessary, since the relevant few theoretical analyses (see, e.g., [16]) employ a number of simplifications and assumptions, which can be useful for a first simple characterization of this problem but look inadequate for reaching a reliable comprehension of the involved phenomena.

In this work, therefore, a synthetic setup is mainly developed, based on an efficient and accurate implementation of a full-wave time-domain CAD simulator, *CST Microwave Studio* [28], [29]: in this way, systematic and wide-ranging parametric analyses are possible, aimed at establishing rigorously what type of functional relations are derivable between the ground permittivity features and significant ETS attributes. In conjunction with related controlled experimental tests through commercial GPR [30], it is, thus, possible to focus on the potentials and criticalities of the ETS technique for an effective evaluation of ground permittivity parameters.

This paper is structured as follows. Section II illustrates the materials and methods, consisting in both experimental (Section II-A) and numerical setups (Section II-B); Section III presents and discusses various reference results on ETS parameterization, both from measurements (Section III-A) and from simulations (Section III-B); Section IV presents concluding remarks and current progress.

II. Materials and Methods

Various accurate investigations on ETS features are possible by varying a number of significant physical parameters, making use of controlled measurements and simulations. In the following, the main features are presented for both laboratory (Section II-A) and numerical setup (Section II-B).

A. Measurements: Experimental Laboratory Setup

The simplest and widely used configuration to investigate the effects on ETS is based on a ground-coupled bistatic GPR system having fixed "close" antennas: i.e., the lateral mutual "offset distance" d is less or comparable to the related signal wavelengths λ (referred to vacuum) in the frequency range of interest. In these "near-field" scenarios, the ETS represents the portion of the signal for which the main wave contributions in the air and ground regions are substantially overlapped at the interface: it is, thus, seen that the ETS can significantly be sensitive to the shallow-soil complex permittivity, involving both real dielectric constant and equivalent conductivity [16], [17].

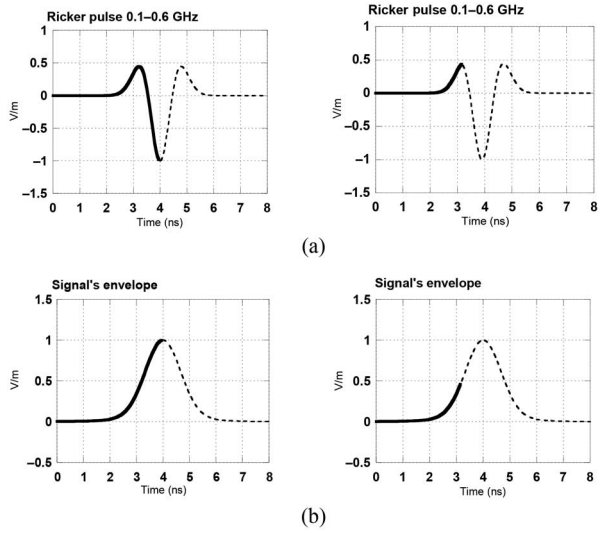

Fig. 1. Typical GPR signals gathered for ETS analysis. (a) Ricker waveform versus time, with its "first half cycle" (bold line in the picture on the left) and "onset" trace (bold line in the picture on the right). (b) Relevant instantaneous "envelope amplitude," again for the "first half cycle" (left) and "onset" trace (right).

For a fully consistent description of such phenomena, it is first necessary to identify the input signal characteristics of the instrument and to establish possibly predictable relationships between gathered signal attributes and medium parameters. In particular, referring to canonical GPR input signal waveforms, such as a Gaussian or a Ricker pulse (as a reference, the latter case is sketched in Fig. 1), it was seen experimentally [16], [17] that, in particular, the "onset" of the first positive half-cycle [Fig. 1(a)] can be the portion of the received signal that exhibits the best correlation with the soil permittivity properties: it results that, in operative scenarios, this choice can indeed maximize the signal-to-noise ratio, by minimizing interference from reflections caused by possible shallow interfaces, clutter, etc. The instantaneous "envelope amplitude" of the first-arrival signal (either the first half-cycle or the onset trace) [Fig. 1(b)], obtained through a Hilbert transform, can, therefore, be chosen as a significant ETS measurable "attribute" to be correlated with the soil EM permittivity [16], [17]. All these discussed quantities are schematically reported in the graphs of Fig. 1.

It should also be reminded that, in such configurations with quite close-coupled antennas, the EM interactions between air and ground waves occur in an extremely complex way, as a function of a number of physical and geometrical parameters. Reliable quantitative studies of the phenomena related to ETS, therefore, require very accurate and extensive procedures of analysis.

A controlled laboratory setup can make use of a GPR commercial instrument equipped with interfacial fixed-offset close antennas, as shown in Fig. 2. In our tests, a *pulseEKKO PRO* with *TR1000* transducer unit by *Sensors & Software Inc.* is used with loaded dipole antennas [30]: a 1-GHz center-frequency system has mainly been chosen here, having a Tx/Rx antenna offset fixed at 7 cm.

The GPR instrument can be placed against the probed ground medium, whose relative dielectric constant and conductivity

Fig. 2. Experimental laboratory setup for the analysis of ETS features. An air/dielectric (glass beads) environment is investigated by means of a simple commercial GPR system with interfacial fixed close antennas. The ground dielectric constant and conductivity can be changed in controllable ways. Proper calibration procedures can be performed on the setup (e.g., a bottom metal plate is located here below the filled box to emphasize the effect of a reflected wave on the gathered signal).

can be changed in controllable way inside a dielectric box (see Section III-A for results of some examples). Suitable calibration procedures of the GPR system have been implemented for test cases in order to have reliable results on measured ETS waveforms. Even though care has to be paid to limit a number of nonideal factors that can adversely affect the reliability of the measurements (e.g., interfacial roughness and inhomogeneity of the media, as well as clutter and noise effects of the environment), GPR signal traces can be gathered and processed.

B. Simulations: Numerical Setup

A "synthetic" numerical setup has been implemented to simulate realistic environments for ETS analysis, based on an efficient EM CAD tool directly operating in the time domain [28], [29]. In the basic GPR configuration of our interest, we are referring to a two half-space region (i.e., generally air for the upper medium and an unknown dielectric for the lower medium), with a fixed ground-coupled Tx/Rx antenna system having "electrically small" mutual separation (in terms of relevant signal wavelengths).

In our synthetic setup, it is possible to design the bistatic antenna configuration, choose the input voltage signal waveforms and, above all, vary the probed medium EM parameters (including loss and dispersive effects). Since, as emphasized, these factors deeply affect the fundamental features of the received signals, the numerical approach gives us the possibility of several efficient, versatile, and inexpensive analyses. As a reference case, a Tx/Rx system is presented here, having interfacial dipole antennas with similar characteristics to the considered commercial GPR system designed to operate at a central frequency of 1 GHz (see a sketch of the simulation environment in Fig. 3).

The reliability of the numerical approach has been tested by using comparisons with measurements and various efficient parametric analyses on ETS are thus possible. Relevant results and discussion are provided in Section III.

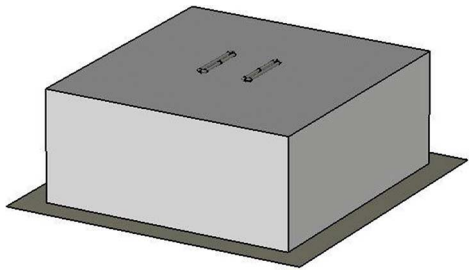

Fig. 3. Synthetic setup based on an EM CAD tool. Implementation of a GPR system for the simulation of ETS. The scenario under analysis consisting of two half-space media (e.g., an air/soil environment, described by the EM parameters ε_r, μ_r, and σ) where a close fixed bistatic ground-coupled Tx/Rx antenna system is located. Resistively loaded folded dipoles are chosen in this case to simulate a commercial GPR antenna system, as that of Fig. 2. A bottom metallic plane is also present here for comparison with a test case on the gathered waveform as in Fig. 2.

III. Results and Discussion

Several types of analysis can be performed in order to assess the influence of different physical and geometrical parameters of the GPR configuration on the ETS features. In the following sections, different specific issues are quantitatively presented and discussed, both experimentally (Section III-A) and numerically (Section III-B).

A. Laboratory Experiments

As said, experimental evidence of the dependence of ETS amplitude on permittivity can be found in various recent works [15]–[27]. Here, we add some considerations concerning the characteristics of the ETS measured waveforms in terms of the dielectric constant (Section III-A1) and of the conductivity (Section III-A2), also useful for comparable simulation results.

1) ETS Characteristics Versus Dielectric Constant: The laboratory controlled experiments enable us to investigate the effects of most critical parameters on the ETS attributes. In order to take this investigation adequately concise, only the main outcomes of the experimental analysis are summarized here, addressing both to the established literature on this issue (see, e.g., [15]–[17], where experimental analyses were performed on the correlation between ETS and permittivity) and to the results of the following sections for parametric studies involving the comparable numerical setup.

The example selected in Fig. 4 refers to our GPR instrument on an air/glass-bead interface ($\varepsilon_r = 3.2$); this ground medium can be considered here as nonmagnetic ($\mu_r = 1$) and lossless ($\sigma = 0$) [28]. The shown received waveform [presented in Fig. 4(a) with dashed lines] is constituted in this case by both a "direct wave" (the effective ETS) and a subsequent strong reflected wave: in fact, in this test case, such contribution is due to the presence of a metallic sheet intentionally placed at the bottom of the filled box for calibration of the experimental setup (see Fig. 2 and further discussion). The fundamental ETS features are anyway identifiable and also allows for proper validation of the synthetic setup as discussed next. Processing on the experimental GPR output is also possible, allowing, for instance, to derive the spectral content of the

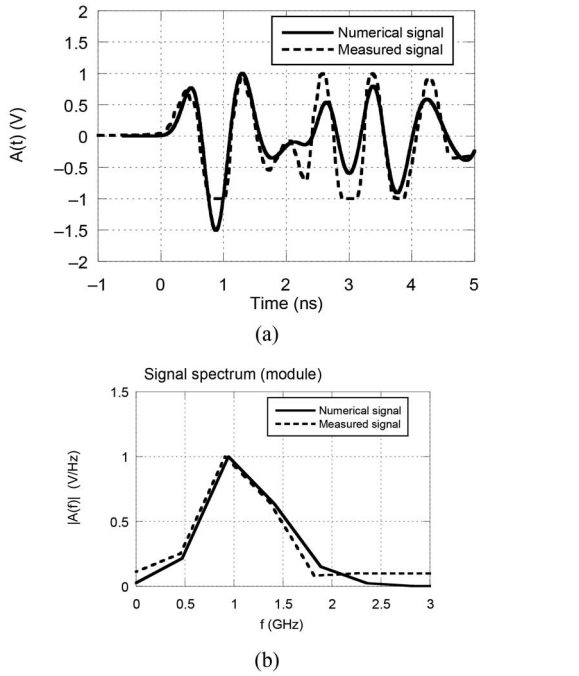

Fig. 4. Behavior of a time-domain signal waveform measured by the GPR in the experimental configuration of Fig. 2, emphasizing the direct wave (ETS contribution) and the first reflected wave due to the presence of a bottom metal sheet. The measured traces are in dashed lines. Comments on additional comparable numerical traces derived by the simulation setup (solid lines) are addressed further. (a) Received waveform (signal voltage amplitude A versus time t), given by a Ricker pulse in an air/glass-bead environment and a metallic reflecting surface on the bottom of the enclosing box. (b) Relevant frequency spectrum of the received signal amplitude: Fourier-transform amplitude versus f (same choice for the style of the lines).

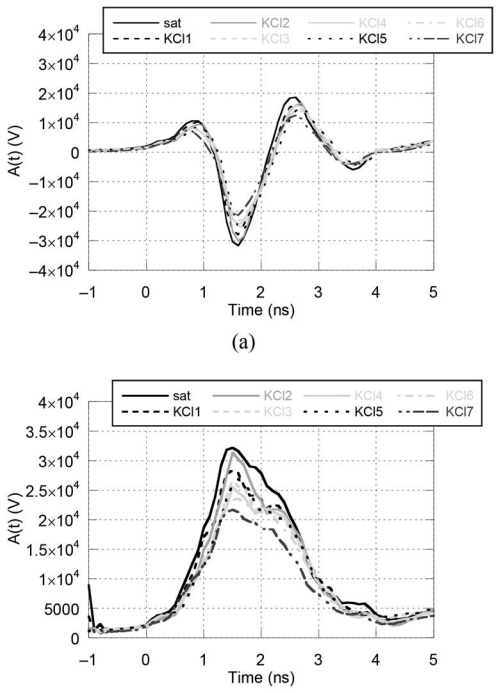

Fig. 5. Measured GPR time-domain ETS traces as a ground granular medium (glass beads) in a saturated water solution ($\varepsilon_r = 29$) changes its conductivity σ by means of different saline *KCl* concentrations. In the legend, the "sat" curve refers to the water-saturated medium without *KCl*, and the curves labeled progressively from "1" to "7" refer to increasing saline concentrations ranging from about 0.4 to 5 g/l, corresponding to linear rise of σ from about 0.006 to 0.21 S/m. (a) Collected ETS traces versus time t. (b) Relevant instantaneous envelope amplitudes versus time t.

gathered ETS waveform by standard Fourier-transform procedures: in Fig. 4(b), the frequency spectrum of ETS is evaluated (dashed line).

The ETS patterns in the time domain are influenced, in particular, by the values of the soil dielectric constant ε_r and of the offset distance d between Tx/Rx antennas. It is experimentally confirmed that, other parameters being fixed, as ε_r increases, the contributions due to the "air" and "ground waves" tend to be progressively more separate, and the ETS becomes no longer representative of the soil medium influence [17]. This strong shape variation of the gathered signal with the separation effect of air and ground waves is also manifest as the antenna offset d is increased, for a fixed value of the soil ε_r (this kind of tests can be performed by means of a GPR instrument having detachable antennas). Such analysis can give a specific indication of which are the basic ranges of variation regarding critical parameters able to make ETS really useful in predicting the soil features.

2) ETS Amplitude Versus Conductivity: The influence of the soil conductivity σ and possible dispersion effects can conveniently be tested with our laboratory setup, keeping conversely fixed the medium dielectric constant ε_r.

As a test case of loss effects on the ETS behavior, expressed in terms of conductivity σ (or, equivalently, of the imaginary part of permittivity), we have considered a granular medium (glass beads) saturated with solutions having different concentrations of potassium chloride (*KCl*), to obtain a bulk σ variable between about 0.006 and 0.21 S/m, with $\varepsilon_r = 29$ (for further details, see [21]). Examples in Fig. 5 present measured signal values versus time for both the gathered GPR traces [Fig. 5(a)] and the relevant envelope amplitudes [Fig. 5(b)], as the saline *KCl* concentration (and therefore σ) varies (in the relevant figure caption and legend, specific information can be found on the different saline concentrations and the related conductivity values).

In these cases, apart from an overall distortion on the gathered trace shape mainly related to dispersion for the presence of the water, it is confirmed that the main effect of increasing losses is just on a relatively limited reduction of the signal amplitude.

B. Simulation Parametric Analysis

The efficiency, flexibility, and economy of the synthetic setup allow us to perform different accurate parametric analyses for ETS. The overall reliability of the numerical approach is first checked (Section III-B1), then the influence of various parameters is studied for the antenna geometry (Section III-B2), the input waveforms (Section III-B3), the dependence of ETS attributes on dielectric constant (Section III-B4), and further parameterization and data fitting (Section III-B5).

1) Check of Synthetic Setup: The results achievable by our CAD implementation have been checked in a number of test cases comparable to the laboratory setup. A comparison is shown for the gathered numerical traces (solid lines) evaluated

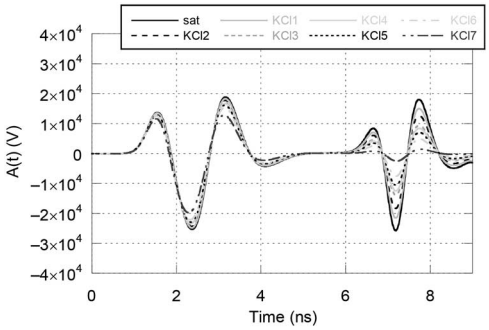

Fig. 6. Simulated time-domain ETS traces as the medium conductivity is varied through different saline concentrations (*KCl*) in a water solution, as in the experiments of Fig. 5. The subsequent time signal replica is related to the location of a bottom metal screen (see Sections II-A and III-A2).

in the experimental scenario (dashed lines) already introduced in Fig. 4(a) for a lossless medium. If we take into account that a number of uncertainties and idealization are present (related to the incomplete knowledge of the specifics of the commercial instrument [30]), the agreement between experiments and simulations looks excellent. The received traces are very well superimposed, as regards time location and amplitude of the ripples, both for the direct ETS portion and for the reflected contribution. In Fig. 4(b), the matching between measured and simulated frequency spectrum of the signal is also remarkable.

As a general observation, it should be pointed out that, in the numerical simulations, the antennas do not include a shielding structure, which is conversely present in the actual configuration of the GPR instrument used for the experimental tests. If such structural information is also available, more realistic simulations can be performed, even though in some cases, the computational burden can become significant. Anyway, it has been tested numerically that, for the "close" Tx/Rx configurations under analysis, the numerical evaluations of the first-arrival signals are not strongly affected by the external shielding structure around the antennas.

The relevant behaviors of simulated traces for the chosen GPR instrument show good matching also if tested for different lossy soils (sand saturated by water with variable saline solutions). The simulated results of Fig. 6 for the synthetic setup agree quite well with the experiments already considered in Section III-A2 (Fig. 5).

2) Influence of the Antenna Geometry on ETS: As anticipated by the experimental analysis, the ETS features are strongly dependent on the permittivity and on the antenna location. This is well confirmed by our numerical analysis. As regards the geometry of the radiating system, it should be emphasized that both antenna mutual distance d ("offset") and interfacial elevation h are parameters extremely important for significant variations of the ETS characteristics.

Representative examples of simulation results are shown considering various Tx/Rx distances d for the loaded dipole antennas simulating the experimental setup of Fig. 2: in the results displayed in Fig. 7, we have evaluated d ranging from 7 to 28 cm with steps of 7 cm. The behaviors of the gathered ETS traces are displayed as the dielectric constant ε_r is also varied, ranging from 3.2 (glass beads of the laboratory setup) to 20. In particular, in Fig. 7(a)–(c), we show the traces for

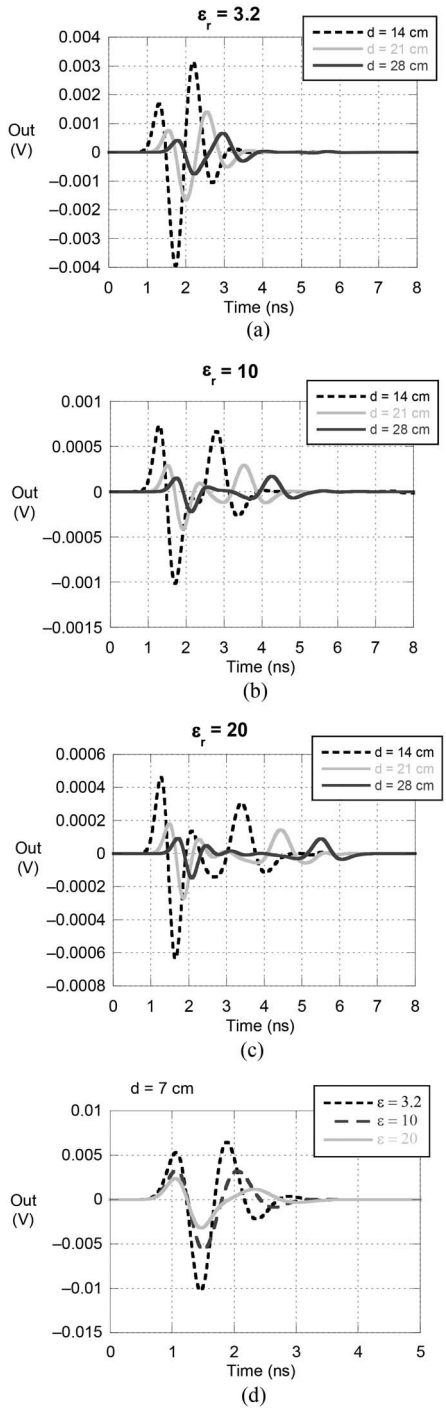

Fig. 7. Received waveforms for a transmitted Ricker pulse analyzed by the numerical model simulating the GPR TR1000 S&S antenna setup. The air-ground wave separation is shown for various offsets d between Tx/Rx antenna and different dielectric constants ε_r. (a) Case of $\varepsilon_r = 3.2$ for three offsets ($d = 14,\ 21,$ and 28 cm). (b) As in (a) for $\varepsilon_r = 10$. (c) As in (a) for $\varepsilon_r = 20$. (d) Case of the lower offset $d = 7$ cm for the same values of dielectric constant ($\varepsilon_r = 3.2,\ 10,$ and 20).

$\varepsilon_r = 3.2,\ 10,\ 20$, respectively (in each case, the offset distance is fixed at $d = 14,\ 21,$ and 28 cm).

From these results, it is confirmed that, being fixed the other parameters, the increasing of the antenna distance d adversely affects the ETS, whose amplitude is rapidly reduced and possibly overwhelmed by nonideal factors (noise, etc.).

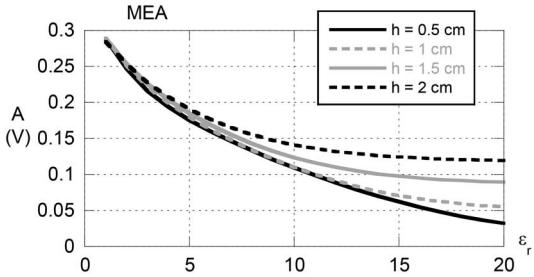

Fig. 8. ETS MEA versus ε_r for the Gaussian modulated pulse, in correspondence with different antenna elevations h from the surface.

The result of Fig. 7(d), summarizing the behavior for the case of the lower offset $d = 7$ cm (with different traces for the same three values of dielectric constant), confirms this trend. It is in fact seen that, by choosing this "small" antenna offset ($d = 7$ cm), the ETS attributes can be quite clearly revealed for ε_r up to about 20, in spite of some progressive shape distortion and amplitude reduction of the gathered waveform.

An additional issue should be emphasized as regards the influence of the antenna geometry on ETS, although so far quite disregarded: in fact, in addition to their offset, even though in ground-coupled configurations, the antennas are very close to the interface, another variable geometrical parameter can deeply affect the amplitude characteristics of the received signal, i.e., the vertical height (elevation) h of the antennas from the surface. The waveforms look very sensitive even to small elevation from the ground, due to the presence of undesired excitation of spurious reflections.

The problem is rather complicated and in this context we show just a representative effect due to this phenomenon. An example of the degree of influence of the antenna elevation h on the ETS attributes is calculated in Fig. 8. It is seen that the curves of the amplitude maintain an overall typical decaying behavior as ε_r increases, and in general tend to rise as h is raised as well (the interval for h is here from 0.5 to 2 cm). This interesting property, possibly related to different coupling effects close to the interface, could be useful in order to improve the sensitivity of the reception in such configurations.

3) Choices of Input Waveforms and Antenna Types: The choice of the input signal waveforms is also related to the characteristics of the antenna type. In connection with the time-domain waveform and relevant spectral features of the chosen signal (Ricker, Gaussian pulse, etc.), the antenna frequency characteristics have to be evaluated in terms of input matching (return loss) and field distribution (radiation patterns).

These aspects are further complicated because, in our scenarios, the system typically works in inhomogeneous environments (i.e., the interfacial antenna features can be sensitively modified by the "loading" due to the subsurface media) and the radiation pattern is not as regular as in far-field conditions (the Tx/Rx antennas can be strongly coupled through involved near-field effects).

As an example, in Fig. 9, we display for a pair of typical pulse signals used in GPR instruments, i.e., a Gaussian modulated pulse [Fig. 9(a) and (b)] and a Ricker pulse [Fig. 9(c) and (d)], both the simulated ETS waveforms (a) and (c) and the relevant envelopes (b) and (d) versus time. These quantities

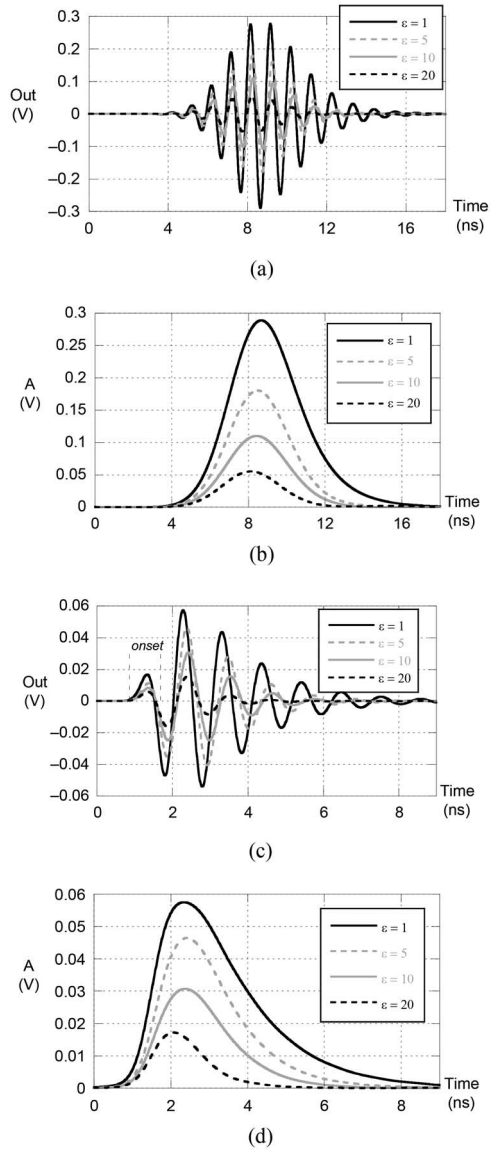

Fig. 9. Simulation results of ETS for a ground-coupled radar system having Tx/Rx $\lambda/2$ dipoles designed at the central frequency $f = 1$ GHz (dipoles fixed with mutual offset $d = 7$ cm and elevation above the interface $h = 1$ cm), using a suitable Gaussian modulated pulse or a Ricker pulse as an input signal. (a) Gaussian pulse: waveforms of the output signal (V) versus time (ns) for a number of different ε_r of the ground medium (see labels): the "onset" and the full "first-arrival" signals are identifiable. (b) Gaussian pulse: relevant overall signal amplitude envelope of the received signal A (V) versus time (ns). (c) Same as (a) for a Ricker pulse. (d) Same as (b) for a Ricker pulse.

are evaluated for different ground dielectric constant ε_r, with a fixed antenna geometry (see also the relevant figure captions). In order to emphasize the influence of the antenna type, these results are derived for a Tx/Rx system based on a pair of simple half-wavelength dipoles (at a center frequency $f = 1$ GHz and an overall bandwidth $BW = 1$ GHz as well). The fact that such radiating elements are basically resonant (if not properly improved in terms of bandwidth through suitable loading or other techniques) is emphasized by marked "ringing" behaviors of the gathered time-domain waveforms in both cases [Fig. 9(a) and (c)].

4) ETS Attributes Versus Dielectric Constant: Based on our synthetic model, in Fig. 10, we illustrate various behaviors

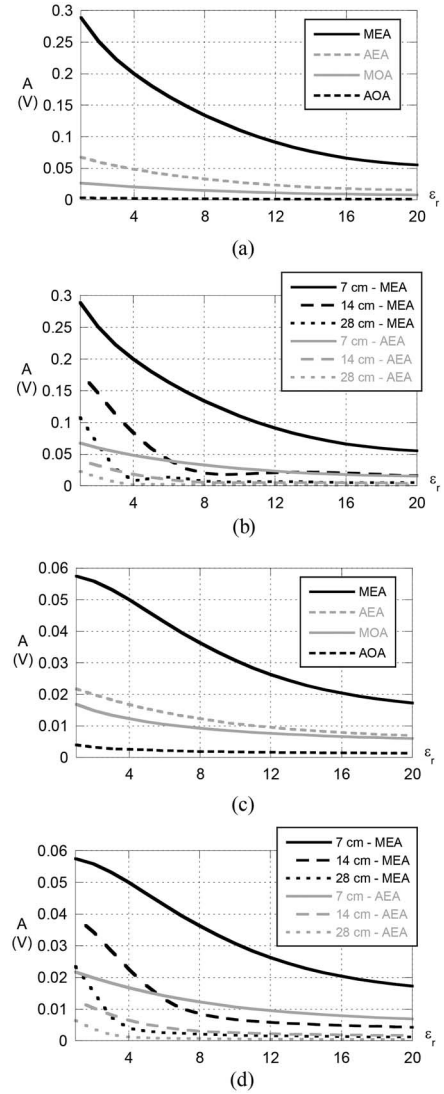

Fig. 10. Simulated results of ETS attributes for a ground-coupled radar system, using a suitable Gaussian modulated pulse or a Ricker pulse as an input signal (see also conditions of Fig. 6). (a) Gaussian pulse: behaviors versus ε_r of the "amplitudes" of "onset" ("-OA") and of first half-cycle "envelope" ("-EA") both for "maximum" ("M-") and for "average" values ("A-"). (b) Gaussian pulse: dependence of the ETS attribute on the antenna offset distance d (fixed elevation $h = 1$ cm): behaviors for the signal "maximum" ("MEA") and "average" ("AEA") "envelope amplitudes" versus ground relative permittivity ε_r, for a selection of different offset values d (see labels). (c) Same as (a) for a Ricker pulse. (d) Same as (b) for a Ricker pulse.

related to the possible choice of different ETS amplitude attributes, as a function of ε_r (the range of values spans continuously between 1 and 20): Fig. 10(a) and (b) reports the results for the Gaussian modulated pulse; Fig. 10(c) and (d) for the Ricker pulse. According to the standard definitions and procedures on ETS (see Fig. 1 and related comments) and referring to the relevant figure captions, in frames (a) and (c), the displayed attributes refer to the ETS amplitudes of the "onset" ("-OA") and of the first half-cycle "envelope" ("-EA"), both for its "maximum" ("M-") and for its "average" values ("A-"). The influence of the antenna offset d is also taken into account in frames (b) and (d) (different curves for $d = 7, 14, \text{ and } 28$ cm).

As a fundamental comment, it is seen that, even though an inverse relationship between early-time amplitudes and

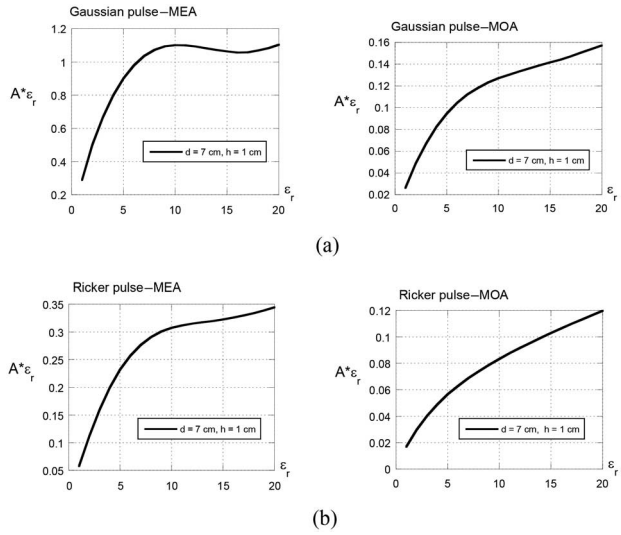

Fig. 11. Functional dependence of the ETS amplitude on dielectric constant. The plots show that the ETS attributes are not a simple function of $1/\varepsilon_r$. (a) Case of the Gaussian pulse (maximum envelope on the left; maximum onset on the right). (b) Same as (a) for the Ricker pulse.

permittivity always occurs, the actual functional dependence between these quantities is not related to simple formulas, as supposed so far [16], [17]. In particular, the dependence of any ETS amplitude A on ε_r is not a simple inverse proportionality (i.e., of the type $1/\varepsilon_r$). This can be verified by plotting as, in Fig. 11, the quantity $A \cdot \varepsilon_r$ as a function of ε_r and noting that this curve is not at all a constant. Only for the envelope peak of ETS and for quite high values of dielectric constant (greater than 10), this simple rule can be seen approximately useful. It is anyway seen that the sensitivity of any attribute drops dramatically as ε_r increases over values of the order of 10.

In spite of the more involved functional relationships recognized between ETS attributes and permittivity, our quantitative analysis can be useful to outline a more precise dependence for such quantities.

It is seen that no simple closed-form expression or "rule of thumb" is possible in the general cases. Nevertheless, based on interpolation procedures of our numerical data, suitable analytical behaviors can be predicted with more accurate formulas, depending on the range of variability of the EM contrast and the other physical parameters of our system. This kind of information is essential to further assess the reliability of the ETS method for practical use if accurate prediction of the EM properties of soils is aimed.

Additional parametric studies have been carried out in order to evaluate also the overall ETS energy in correlation with the dielectric constant and the type of the input pulse. The computation of the ETS energy is obtained by the time integration of the squared signal envelope amplitude of ETS.

An example of this behavior is reported in Fig. 12, again for both Gaussian [Fig. 12(a)] and Ricker [Fig. 12(b)] pulses. The dependence of the signal energy on the dielectric constant is qualitatively similar to what already recognized, even though the rate of decaying is different, as expected. In particular, it is confirmed that the antenna offset d is rather critical, since the amount of energy is quickly decaying when the mutual distance of the antennas increases significantly.

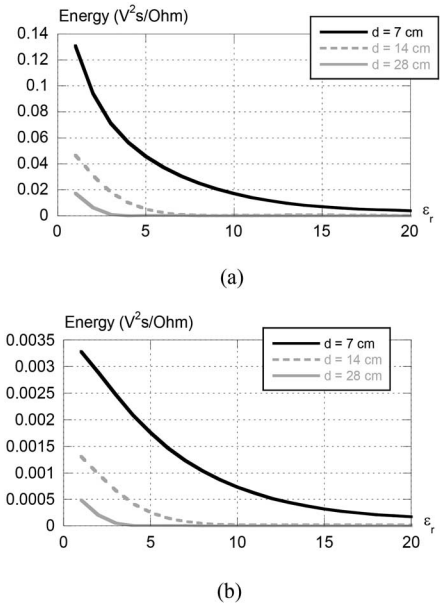

Fig. 12. Evaluation of the energy associated to ETS as a function of ε_r and for different antenna offsets d. (a) Gaussian pulse. (b) Ricker pulse.

5) ETS Frequency Analysis and Data Fitting: Final considerations refer to further promising studies on other "unconventional" observable parameters for possible improvement of the sensitivity of the ETS approach and also on proper derivation of useful interpolation formulas able to well predict these behaviors.

By proper processing the time-domain data of the traces by means of Fourier transform, we have also investigated the amplitude of the received signal carrier frequency as a possible additional ETS observable. Representative examples of the relevance of this specific analysis are provided as a conclusion of the present study, referring both to dielectric constant and to conductivity effects.

If we refer to the spectral content of the signals, it is interesting to monitor the magnitude of the Fourier-transformed (FT) signal at the central operative frequency (what we call here "carrier frequency amplitude," CFA in brief), as a possible descriptive parameter of the main feature of the gathered ETS. This can be easily performed by standard FT processing of the time-domain data (either numerical or experimental ones). It is seen that such alternative attribute presents dependence on the physical and geometrical parameters that is basically similar to those of other observable quantities, but in tested situations the functional relationships look more regular and better predictable. This characteristic can be related to the main signal properties summarized by the carrier frequency, possibly less sensitive to the overall dispersion effects in the investigated scenario.

An example of this study is given in Fig. 13 for data from the synthetic setup. The curves versus dielectric constant are given for the usual ETS envelope and for the carrier amplitude. It is manifest a more regular decaying of CFA as ε_r increases. It is important to note that such consistent behavior makes the derivation of interpolation formulas much simpler. As an example of data fitting, the excellent matching with CFA

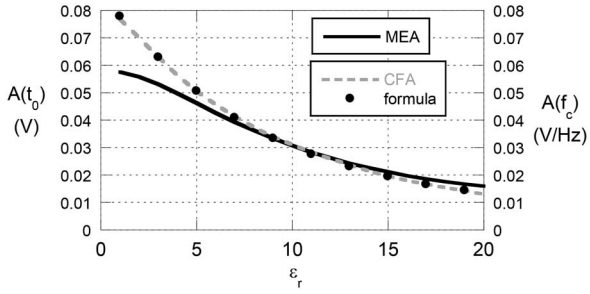

Fig. 13. Simulated behaviors of ETS "alternative" attributes: the CFA versus ε_r. The development of suitable interpolation formulas leads to good fitting and prediction of the ETS.

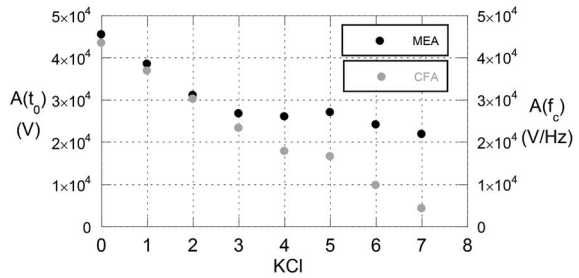

Fig. 14. Evaluation of the measured behavior of the CFA as an alternative ETS observable quantity, compared with the MEA, for a lossy case (different values of a KCl concentration, as in Fig. 5). CFA shows a more regular and wide sensitivity with respect to the conductivity variations.

is also illustrated in Fig. 13, according to an empirical formula as a function of the dielectric constant, given by the following closed-form expression of algebraic type:

$$CFA = \frac{a}{(b + c\varepsilon_r + d\varepsilon_r^2)} \tag{1}$$

where in this case $a = 0.43,\ b = 5,\ c = 0.48,\ d = 0.044$.

In addition to the benefit of achieving valid fitting expressions for the data related to a chosen GPR setup, it should be also emphasized that this method can take advantage of well consolidated approaches that are performed directly in the frequency domain (i.e., in harmonic regime) for canonical Tx/Rx systems of interfacial antennas (particularly, dipoles) [16], [17]. Even though these approaches require various approximations and simplifications, the empirical formulas derived through our numerical study give the significant possibility of testing their degree of accuracy and addressing perspectives for improved functional relationships.

The frequency-domain analysis of ETS traces can be accomplished also for the study of the effects of conductivity. The last example of Fig. 14 refers again to the changes of salt concentration in the porous material discussed in Section III-A2. The carrier amplitude analysis is applied in this case directly to the data from measurements (see Fig. 5). It is interesting to note that, with respect to the already considered maximum envelope amplitude (MEA), the CFA behavior looks again more regularly sensitive to the variation of conductivity, with the consequent considered advantages.

From these results, the analysis of the frequency-domain features of the ETS referred to the carrier can open further

promising perspectives for useful correlation with ground permittivity: such issues look worthy of future devoted theoretical and experimental investigations.

IV. Conclusion

The ETS, which is the first-arrival wave collected by a bistatic ground-coupled radar in simple configurations with close fixed antennas, has extensively been tested as a possible advantageous alternative method for monitoring and mapping the permittivity properties of shallow surfaces at small and intermediate scales.

Suitable experimental and numerical setups have been employed as the most viable strategy for a systematic analysis of this complex topic. Accurate and wide-ranging parametric surveys have thus been presented, starting from basic test studies. For the first time, a comprehensive and reliable view of the most significant issues influencing the practical use of such technique has been quantitatively assessed.

This study has thus allowed us to establish in a rigorous way that, in spite of its conceptual simplicity, the determination of the most effective observable quantities and, above all, the predictability of the relevant functional relationships, represent a rather difficult task to be tackled, depending on various involved and interacting physical and geometrical parameters.

In fact, ETS has shown complex sensitivity on the GPR system configuration (type and location of the antennas, input waveform, and other environmental parameters). Furthermore, it is observed that, as the permittivity values tend to increase, the sensitivity of ETS amplitude strongly decreases and can be easily overwhelmed by strong waveform distortion and environmental uncertainties (noise, clutter, inhomogeneities, etc.). Even though involved coupling phenomena occur between the Tx/Rx antennas, it is, therefore, seen that a "small offset" configuration is generally preferable for ETS clear detection. For a satisfactory accuracy in evaluating dielectric constant and conductivity, initial careful calibration procedures should anyway be required for each specific GPR instrument: e.g., this could imply a number of preliminary test measurements on a set of samples of known permittivity for a chosen GPR to provide the best-fit interpolation of data on dielectric constant and conductivity.

In this connection, the most advantageous choices of ETS attributes have been investigated. Once the signal behaviors as a function of the system parameters are established, suitable empirical interpolation formulas are achievable for the ETS amplitude versus permittivity. Our analysis has also emphasized that, as a completion of this distinguishing time-domain analysis, also spectral data processing can be considered, referring in particular to the signal carrier frequency: this innovative approach looks promising and can deserve specific further investigation.

The results of this analysis can provide a first consistent description both of the potential attractive features and of the critical aspects of the ETS technique. Future research following the strategies delineated in this frame can make this original method increasingly useful in specific operative conditions as a valid alternative to other consolidated approaches.

Acknowledgment

The authors would like to thank Drs. A. P. Annan, A. Di Matteo, and Prof. E. C. Slob, for various useful discussions and interactions on this topic, and also the reviewers for their constructive suggestions and comments.

References

[1] D. J. Daniels (Ed.), *Ground Penetrating Radar*. Piscataway, NJ, USA: IEEE Press, 2004.

[2] H. M. Jol (Ed.), *Ground Penetrating Radar: Theory and Applications*. Amsterdam, The Netherlands: Elsevier, 2009.

[3] P. Annan, "Radio interferometry depth sounding: Part I—Theoretical discussion," *Geophysics*, vol. 38, pp. 557–580, 1973.

[4] P. Annan, "GPR—History, trends, and future developments," *Subsurface Sens. Technol. Appl.*, vol. 3, no. 4, pp. 253–270, Oct. 2002.

[5] R. W. P. King, G. S. Smith, M. Owens, and T. T. Wu, *Antennas in Matter: Fundamentals, Theory, and Applications*. Cambridge, MA, USA: MIT Press, 1981.

[6] J. A. Huisman, S. S. Hubbard, J. D. Redman, and A. P. Annan, "Measuring soil water content with ground penetrating radar: A review," *Vadose Zone J.*, vol. 2, pp. 476–491, 2003.

[7] J. L. Davis and A. P. Annan, "Ground penetrating radar to measure soil water content," in *Methods of Soil Analysis*, J. Dane and G. Topp, Eds. Soil Science Society of America, 2002, pp. 446–463.

[8] K. Grote, S. S. Hubbard, and Y. Rubin, "Field-scale estimation of volumetric water content using ground-penetrating radar ground wave techniques," *Water Resour. Res.*, vol. 39, no. 1321, pp. 1–13, 2003.

[9] L. W. Galagedara, G. W. Parkin, J. D. Redman, P. von Bertoldi, and A. L. Endres, "Field studies of the GPR ground wave method for estimating soil water content during irrigation and drainage," *J. Hydrol.*, vol. 301, no. 1–4, pp. 182–197, Jan. 2005.

[10] S. Lambot, L. Weihermüller, J. A. Huisman, H. Vereecken, M. Vanclooster, and E. C. Slob, "Analysis of air-launched ground penetrating radar techniques to measure the soil surface water content," *Water Resour. Res.*, vol. 42, no. W11403, pp. 1–12, Nov. 2006.

[11] J. A. Huisman, C. Sperl, W. Bouten, and J. M. Verstraten, "Soil water content measurements at different scales: Accuracy of time domain reflectometry and ground-penetrating radar," *J. Hydrol.*, vol. 245, no. 1–4, pp. 48–58, May 2001.

[12] C. Sperl, K. Stanjek, and A. Berktold, "Subsurface moisture determination with the ground wave of GPR," in *Proc. 7th Int. Conf. Ground Penetrat. Radar*, Lawrence, KS, USA, 1998, pp. 675–680.

[13] T. W. H. Caffey, "A range algorithm for ground penetrating radar," in *Proc. Int. Geosci. Remote Sens.*, Lincoln, NE, USA, May 1996, pp. 2023–2026.

[14] S. Lambot, E. C. Slob, I. van den Bosch, B. Stockbroeckx, B. Scheers, and M. Vanclooster, "Modeling of ground penetrating radar for accurate characterization of subsurface dielectric properties," *IEEE Trans. Geosci. Remote Sens.*, vol. 42, no. 11, pp. 2555–2568, Nov. 2004.

[15] E. Pettinelli *et al.*, "Correlation between near-surface electromagnetic soil parameters and early-time GPR signals: An experimental study," *Geophysics*, vol. 72, pp. A25–A28, 2007.

[16] A. Di Matteo, E. Pettinelli, and E. C. Slob, "Early-time GPR signal attributes to estimate soil dielectric permittivity: A theoretical study," *IEEE Trans. Geosci. Remote Sens.*, vol. 51, no. 3, pp. 1643–1654, Mar. 2013.

[17] E. Pettinelli *et al.*, "A controlled experiment to investigate the correlation between early-time signal attributes of ground-coupled radar and soil dielectric properties," *J. Appl. Geophys.*, vol. 101, pp. 68–76, Feb. 2014.

[18] S. Laurens, J. P. Baylassac, J. Rhazi, and G. Arliguie, "Influence of concrete relative humidity on the amplitude of ground-penetrating radar (GPR) signal," *Mater. Struct.*, vol. 35, pp. 198–203, 2002.

[19] Z. M. Sbartaï, S. Laurens, J. P. Baylassac, G. Arliguie, and G. Ballivy, "Ability of the direct wave of radar ground-coupled antenna for NDT of concrete structures," *NDT E Int.*, vol. 39, pp. 400–407, 2006.

[20] C. Ferrara *et al.*, "Comparison of GPR and unilateral NMR for water content measurements in a laboratory scale experiment," *Near Surf. Geophys.*, vol. 11, pp. 143–153, 2013.

[21] C. Ferrara *et al.*, "An evaluation of the early-time GPR amplitude technique for electrical conductivity monitoring," in *Proc. 7th Int. Workshop Adv. Ground Penetrat. Radar (IWAGPR)*, Nantes, France, 2013, p. 4.

[22] D. Comite, A. Galli, C. Ferrara, and E. Pettinelli, "Relations between GPR early-time signal attributes and ground permittivity: A numerical investigation," in *Proc. 8th Eur. Conf. Antennas Propag.*, The Hague, The Netherlands, Apr. 2014, p. 4.
[23] J. D. Redman, G. Hans, and N. Diamanti, "Effect of wood log shape on moisture content measurement using GPR," in *Proc. 15th Int. Conf. Ground Penetrat. Radar (GPR)*, Jun. 2014, pp. 181–185.
[24] N. Diamanti, J. D. Redman, and A. P. Annan, "Importance of simulating realistic transducers in GPR numerical modelling," in *Proc. Near Surf. Geosci.*, 2014, p. 4.
[25] I. Catapano, A. Randazzo, E. Slob, and R. Solimene, "GPR imaging via qualitative and quantitative approaches," in *Civil Engineering Applications Ground Penetrat. Radar*. New York, NY, USA: Springer, 2015, pp. 239–280.
[26] G. Hans, D. Redman, B. Leblon, J. Nader, and A. La Rocque, "Determination of log moisture content using early-time ground penetrating radar signals," *Wood Mater. Sci. Eng.*, vol. 10, no. 1, pp. 112–129, 2015.
[27] G. Hislop, "Permittivity estimation using coupling of commercial ground penetrating radars," *IEEE Trans. Geosci. Remote Sens.*, vol. 53, no. 8, pp. 4157–4164, Aug. 2015.
[28] G. Valerio, A. Galli, P. M. Barone, S. E. Lauro, E. Mattei, and E. Pettinelli, "GPR detectability of rocks in a Martian-like shallow subsoil: A numerical approach," *Planet. Space Sci.*, vol. 62, pp. 31–40, 2012.
[29] (2014). *Users Manual, CST Products*, Germany [Online]. Available: http://www.cst.com
[30] (2014). *Users Manual, Sensors & Software Products*, Canada [Online]. Available: http://www.sensoft.ca

Davide Comite (M'15) received the Master's degree (*cum laude*) in telecommunications engineering and the Ph.D. degree in electromagnetics and mathematical models for engineering from "Sapienza" University, Rome, Italy, in 2011 and 2015, respectively.

His research interests include analysis and design of ground-coupled antennas for geophysical and space applications, study and design of leaky-wave antennas and modal analysis to characterize radiation in planar structures. He is also interested in inverse problems, specifically in the optimization of microwave tomographic algorithms applied to numerical and measured GPR data, considering two-dimensional as well as three-dimensional configurations. His activity also regards techniques of numerical characterization and experimental approaches for the study of electromagnetic subsurface propagation and scattering effects by means of GPR systems.

Dr. Comite was the recipient of the "Marconi Junior 2012" Prize, awarded by "Fondazione Guglielmo Marconi" to Young Student Author of Master Degree Thesis particularly relevant and important in ICT.

Alessandro Galli (S'91–M'96) received the "Laurea" degree in electronic engineering and the Ph.D. degree in applied electromagnetics from "La Sapienza" University of Rome, Rome, Italy, in 1989 and 1993, respectively.

Since 1990, he has been with the Department of Electronic Engineering (now Department of Information Engineering, Electronics, and Telecommunications, DIET), "La Sapienza" University of Rome for his research and educational activities. In 2000, he became an Assistant Professor, and in 2002, an Associate Professor with "La Sapienza" University of Rome, and in 2013, he won the National Scientific Qualification as a Full Professor in the sector of Electromagnetic Fields.

He has authored about 300 scientific works. He is an author of a patent for an invention concerning a type of microwave antenna. His research interests include theoretical and applied electromagnetism, mainly focused on the analysis of microwave passive devices and antennas (leaky-wave structures, waveguiding and radiating components based on multilayered and periodic configurations, metamaterials, graphene, with related modeling and numerical aspects), and on geophysical applications (ground-penetrating radar and time-domain reflectometry techniques); topics of bioelectromagnetics (microscopic interaction mechanisms) and energetics (plasma heating for nuclear fusion).

Dr. Galli was elected as the Italian representative of the Board of Directors of the European Microwave Association (EuMA), the main European Society of Electromagnetics, for the 2010–2012 triennium and then re-elected for the 2013–2015 triennium. In 2014, he was the General Co-Chair of the European Microwave Week (EuMW), the most important conference event at European level on electromagnetics. Since its foundation in 2012, he has been the Coordinator of the European Courses on Microwaves (EuCoM), the first European educational institution on microwaves. He is also a member of the European School of Antennas (ESoA). He is an Associate Editor of the *International Journal of Microwave and Wireless Technologies* (Cambridge University Press) and member of the main international societies on microwaves and antennas. He was the recipient of Barzilai Prize in 1994 for the Best Scientific Work of under 35 researchers at the "10th National Meeting of Electromagnetics" (RiNEm), and the Quality Presentation Recognition Award of the IEEE Microwave Theory and Techniques (MTT) Society at the International Microwave Symposium in 1994 and 1995.

Sebastian Emanuel Lauro received the "Laurea" degree in electronic engineering and the Ph.D. degree in electromagnetics from Roma Tre University, Rome, Italy, in 2005 and 2009, respectively.

His research interests include the study of electromagnetic propagation in metamaterials and the design of microwaves and optic devices.

Dr. Lauro joined the Geophysical Group at Roma Tre University, in 2009, where he is holding his Postdoctoral Fellowship, working on electromagnetic characterization of planetary materials and GPR data inversion for Earth and planetary exploration.

Elisabetta Mattei received the Physics degree (*cum laude*) from "La Sapienza" University of Rome, Rome, Italy, and the Ph.D. degree in environmental physics from the University of Viterbo, Italy, in 2003 and 2007, respectively.

From 2004 to 2007, she was the recipient of various research fellowships on the development of calculator models and investigation through electromagnetic radiation on macro (TDR and radar techniques) and/or micro (visible spectroscopy) scale from the University of Viterbo. Currently, she is a Researcher with the Department of Ecological and Biological Sciences, Università della Tuscia, Viterbo, Italy. In 2008, she was the recipient of a research collaboration on electromagnetic diagnostic through TDR technique at the Department of Physics, Roma Tre University, Rome, Italy. She has been a Contract Professor with the Department of Physics, Faculty of Agriculture and Faculty of Cultural Heritage, University of Viterbo and with the Faculty of Architecture, "La Sapienza" University of Rome. Her research interests include electromagnetic technique for characterization of complex materials, inversion technique through nonlinear fitting and minimization procedure of TDR data using mixing formulas and dielectric models.

Elena Pettinelli received a degree (*cum laude*) in geophysics from the "La Sapienza" University of Rome and the Ph.D. degree in applied geophysics from the University of Trieste, Trieste, Italy, in 1990 and 1993, respectively.

In 1993 and 1994, she was a Visiting Scientist at the University of Waterloo, ON, Canada, where she worked on antenna radiation pattern measurements and GPR response from buried targets. Since 2000, she has been actively involved in Mars subsurface exploration being part of the Science Team of the Ares soil Characterization by Quadrupole Analysis (A.C.QU.A.) Project, supported by the Italian Space Agency (ASI), Rome, Italy. She is a Co-Investigator of the SHARAD experiment and cooperate with the MARSIS Science Team for the electromagnetics laboratory instigations on Martian soil simulants and for radar data inversion. She is also a Co-Investigator and responsible of the Italian Team for the WISDOM radar onboard of the ESA mission EXOMARS, and also Co-Investigator of RIME, the orbiting radar sounder for icy satellites exploration which is part of the payload of the next mission JUICE to the Jupiter Galilean satellites. Currently, she is a Assistant Professor with the Department of Mathematics and Physics, Roma Tre University, Rome, Italy, where she is responsible of the laboratory of "Applied Physics to Earth and Planets." Her research interests include GPR with antenna calibration, target identification, geological, environmental, and archaeological applications.